International Journal of Pharmaceutics 359 (2008) 234–240

Contents lists available at ScienceDirect

International Journal of Pharmaceutics

journal homepage: www.elsevier.com/locate/ijpharm

Pharmaceutical Nanotechnology

Determinants for in vivo anti-tumor effects of PEG liposomal doxorubicin: Importance of vascular permeability within tumors

Ken-ichi Ogawara [a], Keita Un [a], Keiko Minato [a], Ken-ichi Tanaka [b], Kazutaka Higaki [a], Toshikiro Kimura [a,*]

[a] Department of Pharmaceutics, Faculty of Pharmaceutical Sciences, Okayama University, 1-1-1 Tsushima-Naka, Okayama 700-8530, Japan
[b] Department of Clinical Pharmacy, Shujitsu University School of Pharmacy, Okayama 703-8516, Japan

ARTICLE INFO

Article history:
Received 20 November 2007
Received in revised form 25 January 2008
Accepted 15 March 2008
Available online 27 March 2008

Keywords:
Liposome
Doxorubicin
EPR effect
Tumor vasculature
VEGF

ABSTRACT

To elucidate the determinants of the in vivo anti-tumor efficacy of polyethylene glycol (PEG)-modified liposomal doxorubicin (DOX), we examined its anti-tumor effect against three different tumor cell lines (Lewis lung cancer (LLC), Colon-26 (C26) and B16BL6 melanoma (B16)) in vitro and in vivo. In vitro, LLC was the most sensitive tumor to DOX and liposomal DOX based on the MTT assay. However, the strongest in vivo anti-tumor effect was observed in the C26 tumor-bearing mice. The in vivo accumulation of radiolabelled PEG liposome in the C26 tumor after intravenous injection was significantly larger than in other tumors. The extent of vascularity assessed by immunohistochemical staining of CD31 was not directly related with the tumor accumulation of PEG liposome. On the other hand, Evans blue extravasation and secretion of VEGF in C26 tumors were higher than in LLC tumors, clearly demonstrating that the vasculature permeability was higher within C26 tumors. These results indicated that the vascular permeability within the tumor substantially affects the tumor accumulation of PEG liposome and may be one of the important determinants in the in vivo anti-tumor efficacy of PEG liposomal DOX.

1. Introduction

The clinical usefulness of the 3-(4,5-dimethylthiazol-2-yl)-2,5-diphenyl tetrazolium bromide (MTT) assay-based in vitro chemosensitivity test is widely recognized to predict patient responses to particular drugs, allowing for the selection of appropriate chemotherapeutic drugs and the avoidance of ineffective drugs, thereby improving patient survival (Tonn et al., 1994; Nakamura et al., 2006). Accumulating knowledge on this assay revealed its usefulness especially to avoid the administration of ineffective chemotherapeutic drugs to patients. However, there are papers reporting the false-positive results of MTT assay-based selection of drugs (Smit et al., 1992; Kratzke and Kramer, 1996; Shaw et al., 1996). These results indicate that not only the in vitro sensitivity of tumor cells isolated from patients toward a given chemotherapeutic drug but also the in vivo disposition characteristics of the drug including its accessibility to tumor tissue would be the important determinants for the therapeutic outcome in the cancer chemotherapy.

Most solid tumors possess unique pathophysiological characteristics that are not observed in normal tissues/organs, such as extensive angiogenesis, defective vascular architecture and impaired lymphatic drainage/recovery system. Generally, the capillary permeability of the endothelium in newly vascularized tumors is significantly greater than that of normal organs. Many of drug delivery approaches to target tumors take advantage of these unique pathophysiological properties of tumor vasculatures (Maeda et al., 2000). Due to the long circulation time of polyethylene glycol (PEG)-modified liposomes (PEG liposome) and the leakiness of the microcirculation in the solid tumors, PEG liposome containing anticancer drugs has been shown to accumulate preferentially in the tumors (Unezaki et al., 1996; Gabizon et al., 2006; Heyes et al., 2006). This phenomenon known as the enhanced permeability and retention (EPR) effect has been generally observed in many types of solid tumors and provides a great opportunity for passive targeting of liposomal anticancer agents into the tumor tissue (Northfelt et al., 1998; Schmidt et al., 1998). PEG liposomal doxorubicin (Doxil®, Caelyx®) has been approved for the treatment of several types of cancers in Japan, U.S. and Europe. However, the extent of vascularity and permeability of vasculatures within tumors might be different from one tumor to the other. Therefore, these pathophysiological differences in the tumor may result in the different therapeutic effects in the EPR effect-based therapy. In the present study, we prepared the different tumor-bearing mice models (colon adenocarcinoma, C26; Lewis lung cancer, LLC; and B16BL6 melanoma, B16) and analyzed these pathophysiological

* Corresponding author. Tel.: +81 86 251 7948; fax: +81 86 251 7926.
E-mail address: kimura@pharm.okayama-u.ac.jp (T. Kimura).

0378-5173/$ – see front matter © 2008 Elsevier B.V. All rights reserved.
doi:10.1016/j.ijpharm.2008.03.025

characteristics of each tumor. Therapeutic effect of intravenously administered PEG liposomal doxorubicin (DOX) was also evaluated in these tumor-bearing mice models to find out determinants for the EPR effect-based in vivo anti-tumor effects of PEG liposomal DOX including the in vitro sensitivity of these tumor cells to DOX.

2. Materials and methods

2.1. Materials

Distearoyl phosphatidylethanolamine-*N*-[methoxy poly (ethylene glycol)-2000] (PEG-DSPE) and hydrogenated soybean phosphatidylcholine (HSPC) were purchased from NOF Inc. (Tokyo, Japan). Cholesterol (Chol) and [^{3}H] Cholesteryl hexadecyl ether ([^{3}H] CHE) were purchased from Wako Pure Chemical Industry Inc. (Osaka, Japan) and PerkinElmer Life Science Inc. (Boston, MA, USA), respectively. Doxorubicin (DOX), 3-amino-9-ethylcarbazole (AEC) tablets and 3-(4,5-dimethylthiazol-2-yl)-2,5-diphenyltetrazolium bromide (MTT), Dulbecco's modified Eagle's medium (DMEM), RPMI, fetal bovine serum (FBS) and antibiotics were obtained from Sigma (St. Louis, MO, USA). Rat anti-mouse CD31 or rat anti-mouse vascular endothelial growth factor (VEGF) antibody was purchased from BD Biosciences (San Jose, CA, USA) or from R&D Systems (Minneapolis, MN, USA), respectively. Horse radish peroxidase (HRP)-conjugated rabbit anti-rat IgG or goat anti-rabbit IgG was purchased from Zymed Laboratory (San Francisco, CA). All other chemicals were of the finest grade available.

2.2. Cells

LLC, C26 and B16 were kindly provided from Cell Resource Center for Biomedical Research, Institute of Development, Aging and Cancer, Tohoku University (Sendai, Japan). LLC was cultured in DMEM, and C26 or B16 was cultured in RPMI, both supplemented with 100 U/ml penicillin, 100 μg/ml streptomycin, 20 μg/ml gentamicin and 10% heat-inactivated FBS at 37 °C under 5% CO_2/95% air.

2.3. MTT assay

Sensitivity of each type of tumor cells to DOX was evaluated using 3-(4,5-dimethylthiazol-2-yl)-2,5-diphenyltetrazolium bromide (MTT)-based cytotoxicity assay (Mosmann, 1983). Briefly, cell suspension diluted with the corresponding growth medium was added to each well (3000 cells/well) of a 96-well flat bottom microtitration plate (Asahi Techno Glass, Chiba, Japan). All plates were incubated for 12 h at 37 °C in a humidified 5% CO_2 atmosphere. Nine dilutions (0.01–100 μM) of DOX solution or PEG liposomal DOX were added to each corresponding wells in the plate. After incubation for 48 h, each well was washed and rinsed with growth medium. MTT solution (5 mg/ml) was added to each well and the cultures were further incubated for 4 h at 37 °C. The medium containing MTT was removed from the wells and the remaining MTT-formazan crystals were dissolved by adding 100 μl of 0.04 M HCl–isopropanol. After being subjected to sonication in a bath-type sonicator (ASONE Corporation, Osaka) for 15 min, each plate was set into an ELISA plate reader (Bio-Rad, Hercules, CA) and absorbance at 570 nm (test wavelength) and 750 nm (reference wavelength) were simultaneously measured. The absorbance at reference wavelength was subtracted from the absorbance at test wavelength. Results were expressed as percent cell survival, calculated for each DOX concentration by the following formula:

$$\%\,\text{cell survival} = \frac{\text{OD}_{570,\text{sample}} - \text{OD}_{750,\text{sample}}}{\text{OD}_{570,\text{control}} - \text{OD}_{750,\text{control}}} \times 100 \quad (1)$$

where sample and control mean the cells with and without DOX treatment, respectively. Percent cell survival was plotted against DOX concentration and was fitted with the Hill-type equation (Eq. (2)) (Eghbali et al., 2003; Lim et al., 2004) using the non-linear least-squares regression program MULTI (Yamaoka et al., 1981). The concentration at which 50% of cells survived corresponded to IC_{50}:

$$E = \frac{E_0 \times \text{IC}_{50}}{\text{IC}_{50} + C} \quad (2)$$

where E or E_0 is the % cell survival with or without DOX treatment, respectively, and C is the final concentration of DOX in each well. Each experiment was performed using three replicated wells for each DOX concentration and carried out independently five times.

2.4. Liposome preparation

Liposomes were prepared as follows. Lipids from chloroform stock solution of HSPC, Chol, and PEG-DSPE were mixed (HSPC:Chol:PEG-DSPE = 56:38:5 by molar ratio) with trace amount of [^{3}H] CHE, and dried under reduced pressure. For liposomes without DOX, the dried lipid film was hydrated with PBS (pH 7.4) under mechanical agitation. Then, the resulting multilamellar preparations were sized by repeated extrusion through polycarbonate membrane filters (Millipore, Bedford, MA, USA) with the pore size of 200 nm followed by further extrusion through the one with 100 nm. For the preparation of DOX-containing liposome, DOX was encapsulated by remote loading method (Haran et al., 1993). In short, after the dried lipid film was hydrated with 250 mM ammonium sulfate (pH 5.4), the resulting liposomes were passed through a Sephadex G-25 column equilibrated with PBS (pH 8.0) to change the pH of the external phase. DOX in PBS (pH 8.0) was added to liposomes at a drug-to-lipid molar ratio of 1:10 and incubated at 60 °C for 1 h. Our preliminary experiments showed that DOX was efficiently encapsulated into liposomes and the loading efficacy was more than 98% reproducibly. Particle sizes of the liposome were determined by dynamic light scattering spectrophotometer (DLS-7000, Otsuka Electronics, Osaka), and were 94.7 ± 9.4 nm and 96.4 ± 14.8 nm for the empty liposome and DOX-containing liposome, respectively.

2.5. Tumor-bearing mice model

Male BALB/c or C57BL6 mice (6–7 weeks) for the inoculation of C26 or LLC and B16, respectively, were purchased from Charles River Laboratories Inc. (Yokohama, Japan) and maintained at 25 °C and 55% of humidity with free access to standard chow and water. To prepare tumor-bearing mice, 1 million tumor cells were subcutaneously injected in the back of mice. Our investigations were performed after approval by our local ethical committee at Okayama University and in accordance with Principles of Laboratory Animal Care (NIH publication #85-23).

2.6. Tissue distribution

Liposome (10 μmol total lipid/kg) containing trace amount of ^{3}H-CHE was intravenously administered into tumor-bearing mice when the tumor grew up to 500 mm^3 in volume. At 48 h after injection, various organs including the liver, spleen, lung, kidney, heart and tumor were excised for the measurement of radioactivity after washed with saline. To solubilize organs, Soluene-350 (Packard instrument Inc., Meriden, CT, USA) was added and incubated for 2 h at 50 °C before neutralized by HCl. Scintillation medium was added to samples, and radioactivity was determined by a liquid scintillation counter (TRI-CARB® 2260XL, Packard instrument Inc.).

2.7. In vivo anti-tumor activity

When the tumor grew up to 500 mm^3 in volume, DOX-containing liposome was administered at a dose of 5 mg/kg DOX by intravenous injection through the tail vein. Saline solution was injected into control group. The tumor volume was measured every other day with a caliper in two dimensions, and was calculated using the following equation: volume (mm^3) = longer diameter × (shorter one)^2 × 0.52 (Lee et al., 2005). The results were expressed as % of initial volume for all tumor models. The experiment was terminated when one of the mice in either control or treatment group died. A slope of % of initial volume–time curve, representing the growth rate of each tumor in the treatment group (T), was obtained (day 11–18, 11–24, or 14–28 for LLC, C26, or B16 tumor, respectively) and divided by that in the control group (C) to give an index (T/C) for the in vivo therapeutic effect for each tumor-bearing mouse model.

2.8. Immunohistochemical staining of CD31 or VEGF within the tumor tissue

Tumor tissues were excised from mice when the tumor grew up to 500 mm^3 in volume and snap-frozen in isopentane. Acetone-fixed 5-μm thick sections of tumor tissues were prepared with the use of cryostat (CM1850, Leica Microsystems, Wetzlar, Germany). Then, the tumor sections were incubated with rat anti-mouse CD31 antibody or VEGF antibody diluted in PBS containing 5% FBS. This was followed by incubation with horse radish peroxidase (HRP)-conjugated rabbit anti-rat IgG antibody and further incubation with HRP-conjugated goat anti-rabbit IgG antibody. Peroxidase visualization was performed by the conventional staining procedure with 3-amino-9-ethyl-carbazole (AEC, Sigma), and the sections were counterstained with Mayers hematoxylin (Merck, Darmstadt, Germany) according to standard laboratory protocols. In the case of CD31 staining, the staining procedure was followed by the counting of the number of vessels under the microscope in ten independent fields for each type of tumor cells.

2.9. Extravasation of albumin-Evans blue within tumor tissues

Evans blue dissolved in saline (1 mg/mL) was administered into the tail vein of tumor-bearing mice at a dose of 4 mg/kg. Forty-eight hours after intravenous injection, tumors were excised and were snap-frozen. Cross-sections of tumor tissues were prepared as described above and were directly subjected to the observation under the microscope equipped with digital recording system (VH-5000, KEYENCE, Osaka).

2.10. Enzyme-linked immunosorbent assay for VEGF

Tumor tissues with 500 mm^3 in volume were homogenized in lysis buffer containing 5% protease inhibitor cocktail (Sigma). VEGF levels were quantified with commercially available enzyme-linked immunosorbent assays (Mouse VEGF ELISA kit, BioSource International, Inc., Camerillo, CA).

2.11. Statistical analysis

Results are expressed as the mean ± S.D. Analysis of variance (ANOVA) was used to test the statistical significance of differences among groups. Statistical significance was evaluated by using Student's *t*-test or Dunnett's test for the single or multiple comparisons of experimental groups, respectively.

3. Results and discussion

To have an optimal in vivo anti-tumor effect in the cancer chemotherapy, many factors that influence the therapeutic outcome should be taken into consideration. Among them, the sensitivity of tumor cells composing a tumor tissue against the anticancer drug used is one of the most important factors. Irrespective of the approaches to improve the drug delivery into tumor tissues, the tumor cells with very low sensitivity to a given anticancer drug will not be efficiently killed with the drug. On the other hand, it was reported that anticancer drugs with high sensitivity did not always lead to the good therapeutic outcome (Smit et al., 1992; Kratzke and Kramer, 1996; Shaw et al., 1996).

In the present study, to elucidate the important determinants for the EPR effect-based in vivo anti-tumor effect of PEG liposomal DOX, we first evaluated the sensitivity of each type of tumor cells tested to DOX solution (Fig. 1a). The obtained results revealed that LLC had the smallest IC_{50} value (0.096 μM) among the three tumor cells studied, indicating that LLC was the most sensitive to DOX solution. B16 tended to show the larger IC_{50} value (0.213 μM) than LLC, and C26 showed significantly larger IC_{50} value (0.311 μM) than LLC, suggesting the lower sensitivity to DOX. We also performed the similar study using PEG liposomal DOX (Fig. 1b). It was confirmed that the order of sensitivity of the three tumor cells was the same as that for DOX solution and C26 showed significantly larger IC_{50} value

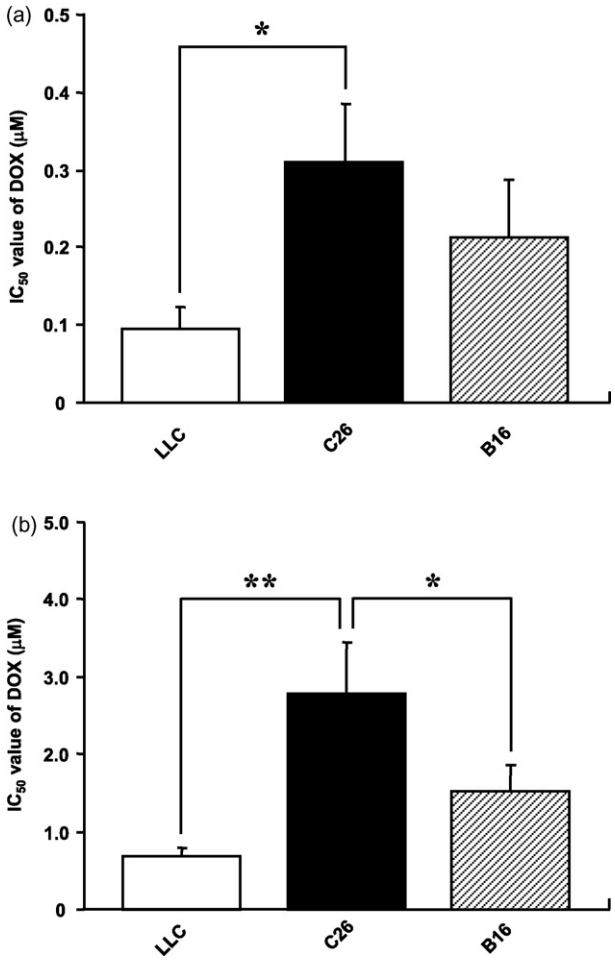

Fig. 1. In vitro sensitivity of Lewis lung cancer (LLC), Colon-26 (C26) and B16BL6 melanoma (B16) cells to DOX solution (a) and PEG liposomal DOX (b). Results are expressed as the mean with the vertical bar showing S.D. of five independent experiments. $^{**}p < 0.01$, $^{*}p < 0.05$.

Table 1
Tumor growth rates and T/C values in tumor-bearing mice

	Tumor growth rate (% of initial/day)		T/C
	Control (saline)	PEG liposomal DOX	
LLC	205 ± 72	51.8 ± 18.0*	0.35 ± 0.09#
C26	37.6 ± 8.9	2.71 ± 7.47***	0.07 ± 0.20
B16	123 ± 37	57.2 ± 33.2 *	0.46 ± 0.27#

Tumor growth rate was estimated as the slope of tumor growth-time curve calculated based on day 11–18, 11–24, or 14–28 for LLC, C26, or B16 tumor, respectively. T/C values were calculated as the ratio of PEG liposomal DOX treated- to control groups in tumor growth rate.

* $p < 0.05$.

*** $p < 0.001$, compared with each control group.

# $p < 0.05$, compared with C26.

than other tumor cells, suggesting the lowest sensitivity to DOX. The absolute IC_{50} values for PEG liposomal DOX (LLC, 0.68 μM; C26, 2.5 μM; B16, 1.4 μM) were about 10 times larger than DOX solution, reflecting the slow release rate of doxorubicin from PEG liposome.

In vivo anti-tumor effect of PEG liposomal DOX was also studied in the mice bearing C26, LLC or B16 tumor (Fig. 2 and Table 1). Significant in vivo anti-tumor effects of liposomal DOX were observed in all the tumor models studied. On the day when we terminated the experiment, the size of C26 tumor treated with liposomal DOX was much smaller (around 200% of the initial volume) than other tumors investigated (Fig. 2). Since the tumor growth rate was different depending on the type of tumors, we also calculated the index for the in vivo therapeutic effect (T/C) that is independent of the growth rate of each type of tumors, to compare the in vivo efficacy of liposomal DOX and were summarized in Table 1. Calculation of T/C also gave the significantly lower value (0.07 ± 0.20) for C26 tumor-bearing mice than other two tumors (LLC, 0.35 ± 0.09; B16, 0.46 ± 0.27). From these results, it was revealed that the strongest in vivo anti-tumor effect was observed in the C26 tumor model, and that the in vivo anti-tumor effect of PEG liposomal DOX was not directly reflecting the sensitivity of tumor cells against DOX.

The in vivo disposition characteristics of intravenously administered PEG liposome must be taken into considerations as one of the crucial factors for the therapeutic outcome of PEG liposomal DOX. It was reported that DOX injected as a solution was so rapidly eliminated from plasma by being excreted into bile and urine and that the amount of DOX distributed into tumor tissues was very small (Gabizon et al., 1996; Mayer et al., 1989). PEG liposomal preparation can improve the retention of DOX in plasma, but to exert the in vivo anti-tumor effect of PEG liposomal DOX, certain amount of DOX-containing PEG liposome must be extravasated to get into the tumor tissue, and DOX must be released and taken up by the surrounding tumor cells. In plasma, DOX leakage from the liposome with the same lipid composition as those applied in this study was very slow ($T_{1/2} = 100$ h) and the presence of fluid obtained from malignant effusions significantly elevated the release rate (Gabizon, 1995). Therefore, DOX would be mainly released from PEG liposome after the liposome is extravasated within the tumor tissue. Considering the low leakage of DOX from PEG liposome in the blood circulation, the in vivo disposition characteristics of PEG liposomal DOX would be similar to the one of PEG liposome. Therefore, we evaluated the in vivo distribution characteristics of ^{3}H-labeled PEG liposome by measuring radioactivity.

Tissue distribution of PEG liposome at 48 h after intravenous administration was investigated in the mice bearing C26, LLC or B16 tumor of 500 mm^3 in volume (Fig. 3). Tissue distribution of PEG liposome exhibited the similar tendency for each tumor-bearing mice, and it was found that PEG liposome mainly distributed to the liver and spleen irrespective of the type of tumors. On the other hand, the distribution of PEG liposome into tumor was quite different depending on the type of the tumors used, and the disposition amount of PEG liposome in the C26 tumor was significantly and approximately threefold larger than those in the other two tumors. These results suggest that the tumor accumulation of PEG liposome correlates with the in vivo anti-tumor efficacy of PEG liposomal doxorubicin in these tumors.

After its systemic administration, the liposome follows two distinct processes before its accumulation into tumors, i.e., circulation within vessels (blood circulation) and transport across vasculature walls into the surrounding tumor tissues (extravasation). Generally, extravasation of particles in blood circulation is a function of both local blood flow and vascular permeability. One of the factors that influence the local blood flow is the extent of vascularity within the tissue. That is to say, the tissue with numerous vasculatures will receive larger local blood supply. To unravel the mechanism underlying the larger tumor accumulation of PEG liposome in C26 tumor, we evaluated the extent of vascularity in each type of tumor tis-

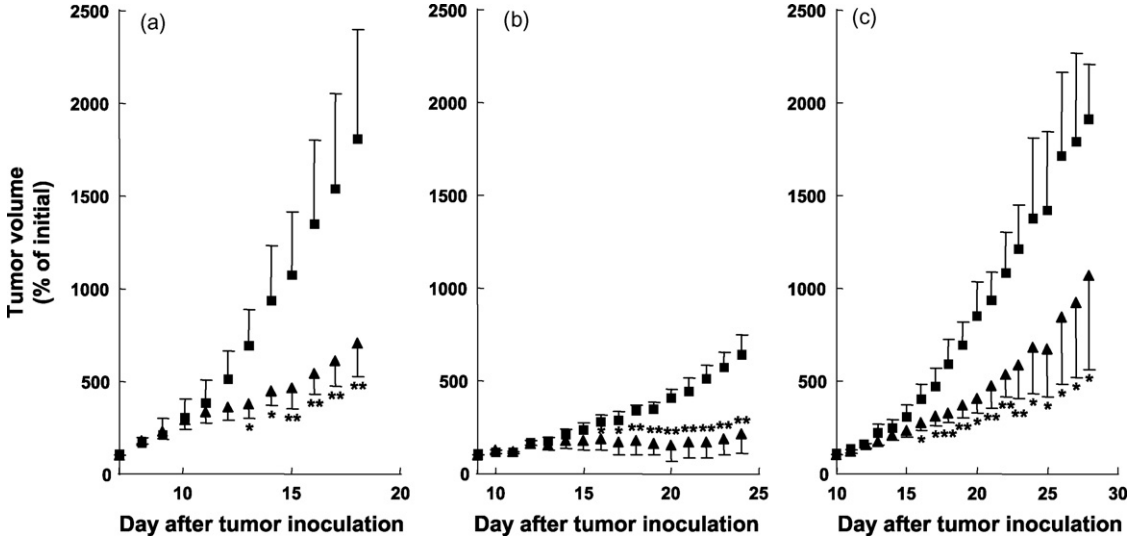

Fig. 2. In vivo anti-tumor effect of PEG liposomal DOX in tumor-bearing mice. Tumor volume was expressed as % of initial volume (around 500 mm^3) for all tumor models. Results are expressed as the mean with the bar showing S.D. of five experiments. *$p < 0.05$; **$p < 0.01$, compared with saline treatment. (a) LLC-bearing mice; (b) C26-bearing mice; (c) B16-bearing mice. Keys: (■) saline treatment; (▲) PEG liposomal DOX treatment. DOX dose was 5.0 mg/kg.

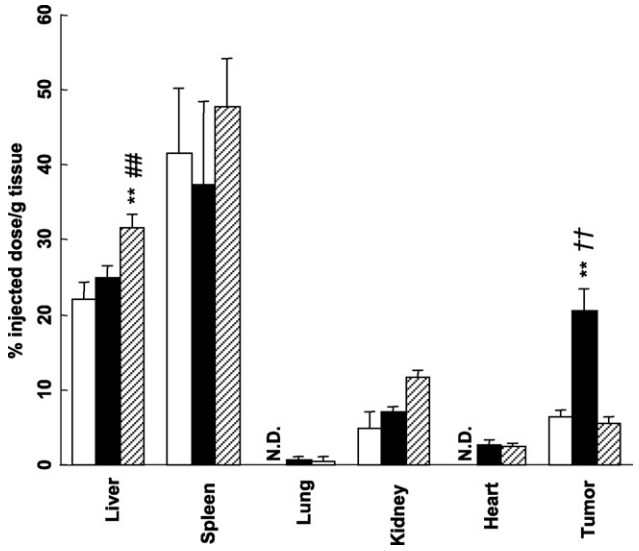

Fig. 3. Tissue distribution of PEG liposomes at 48 h after intravenous administration into tumor-bearing mice. Keys: (□) LLC-bearing mice; (■) C26-bearing mice; (▨) B16-bearing mice. Results are expressed as the mean with the bar showing S.D. of three experiments. $^{**}p < 0.01$, compared with LLC-bearing mice; $^{\#\#}p < 0.01$, compared with C26-bearing mice; $^{\dagger\dagger}p < 0.01$, compared with B16-bearing mice. Dose of liposome was 10 μmol total lipid/kg.

sue. To visualize the vasculature, cryostat sections were incubated with rat antibody recognizing the mouse endothelial cell marker CD31, followed by the standard staining procedure as described in Section 2. As shown in Fig. 4, in the sections prepared from LLC and B16 tumors, tube-like large vessels were often observed but the numbers of vessels were relatively small (LLC, 28 ± 5; B16, 17 ± 6 vessels per field). On the other hand, a lot of tiny vessels (47 ± 6 vessels per field) equally distributed throughout the tumor tissue were observed in C26 tumor.

Besides the extent of vascularity, the permeability of vasculature within the tumor tissue would be one of the important factors influencing the transport of liposome across vasculature walls (Yuan et al., 1995) and may vary considerably depending on the type of tumor models. Several earlier studies demonstrated the differences in the vascular permeability of macromolecules among the tumor tissues used (Graff et al., 2000, 2001; Dreher et al., 2006). Evans blue was utilized to evaluate the vascular permeability of tumor tissues, because the dye spontaneously makes a complex with serum albumin by electrostatic interaction between the sulfonic acid group of the dye and the terminal cationic nitrogens of the lysine residues of albumin (Clasen et al., 1970) and it has, therefore, been generally applied to evaluate the vascular permeability within tumor tissues (Amice et al., 1978; Roberts and Hasan, 1993; Tanaka et al., 2003). Since it was previously reported that the amount of Evans blue remaining in the blood is negligible at 48 h after its intravenous administration at 10 mg/kg (Graff et al., 2000), we excised tumor tissues at 48 h after intravenous administration in order to discriminate Evans blue extravasated from that in blood vessels. In C26 tumor, the blue color derived from Evans blue was able to be clearly observed equally throughout the tumor (Fig. 5b), suggesting that the permeability of vasculature within C26 tumor would be high and the equal distribution of tiny vasculature throughout the tumor would also be responsible for this observation. On the other hand, in the case of LLC tumor, the blue color was hardly found (Fig. 5a), indicating that the permeability of vasculatures in LLC tumor is very low and that the vascularity is not necessarily a sufficient factor for the efficient intra-tumoral accumulation of PEG liposome. Unfortunately, we were not able to perform the similar study for B16 tumor due to the intrinsic black color of the tissue. Although we did not see any direct relationship between the extent of vascularity (Fig. 4) and the tumor accumulation characteristics of PEG liposome (Fig. 3), the results on Evans blue extravasation obtained for C26 and LLC tumors (Fig. 5) could explain the difference in the tumor accumulation of PEG liposome between the two tumor tissues. That is to say, not only the extent of vascularity within the tumor but also the vascular permeability would be responsible for the accumulation of PEG liposome into tumor tissues. Therefore, the vascular permeability within the tumor would be one of the crucial determinants in the in vivo anti-tumor effect of PEG liposomal DOX. To draw more universal conclusion on this issue, however, increasing the number of tumor types investigated would be necessary and will be the subject of our further study. In addition, intra-tumoral distribution pattern of PEG liposome would also be an important factor to determine the in vivo anti-tumor effect. Although we did not directly evaluate the intra-tumoral distribution of PEG liposome, we consider that the intra-tumoral distribution of extravasated Evans blue would be reflecting that of PEG liposome. Therefore, it can be considered that the higher permeability of vasculature and the equal distribution of tiny vasculature observed in the case of C26 tumor would be beneficial for the efficient intra-tumoral distribution of PEG liposome. Together with these factors, the difference in the extent of vascularity between central and peripheral parts of tumor tissue and/or the interstitial fluid pressure may vary depending on the type of tumor and would affect the intra-tumoral distribution of PEG liposome.

One of the major factors that influence the vascular permeability within the tumor tissue is VEGF (Kliche and Waltenberger, 2001). To unravel the mechanism underlying the difference in vascular permeability between C26 and LLC tumors, we performed immunohistochemical staining of VEGF within the tumor tissues for the semi-quantification (Fig. 6a and b). As shown in Fig. 6a and b, the higher amount of VEGF in C26 tumor than LLC tumor was detected. Furthermore, the quantification of VEGF amount in each tumor by ELISA demonstrated that approximately eightfold larger

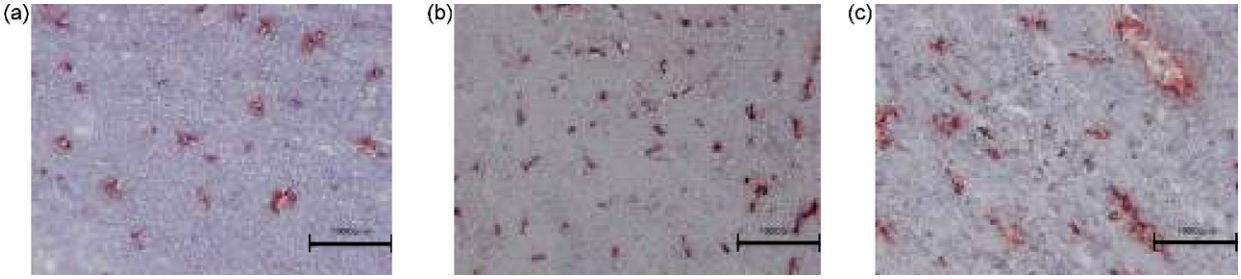

Fig. 4. Immunohistochemical staining of CD31 in each tumor section of LLC (a), C26 (b), and B16 tumors (c). Tumor tissues were excised from mice when the tumor became 500 mm^3 in volume and were snap-frozen. Acetone-fixed 5-μm thick sections of tumor tissues were prepared and then AEC staining was performed for CD31 as described in Section 2. Bar: 100 μm.

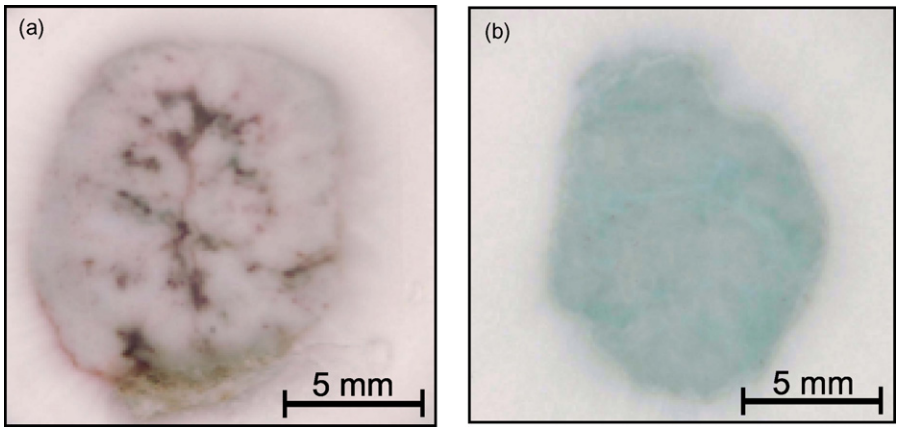

Fig. 5. Extravasation of Evans blue in LLC (a) and C26 tumors (b). Forty-eight hours after intravenous injection of Evans blue solution, tumors were excised and were snap-frozen. Cross-sections of tumor tissues were directly subjected to the observation under the microscope as described in Section 2. The result shown here is the representative one among three independent tumor sections per group.

amount of VEGF was secreted in C26 tumor compared with that of LLC tumor (Fig. 6c). From these results, it was suggested that the higher vascular permeability within C26 tumor (Fig. 5) would be ascribed to its higher secretion of VEGF within the tumor tissue. Mediators that would be substantially responsible for enhancing the secretion of VEGF in these tumor tissues remain unclear, but should be identified for the development of the more efficient cancer chemotherapy.

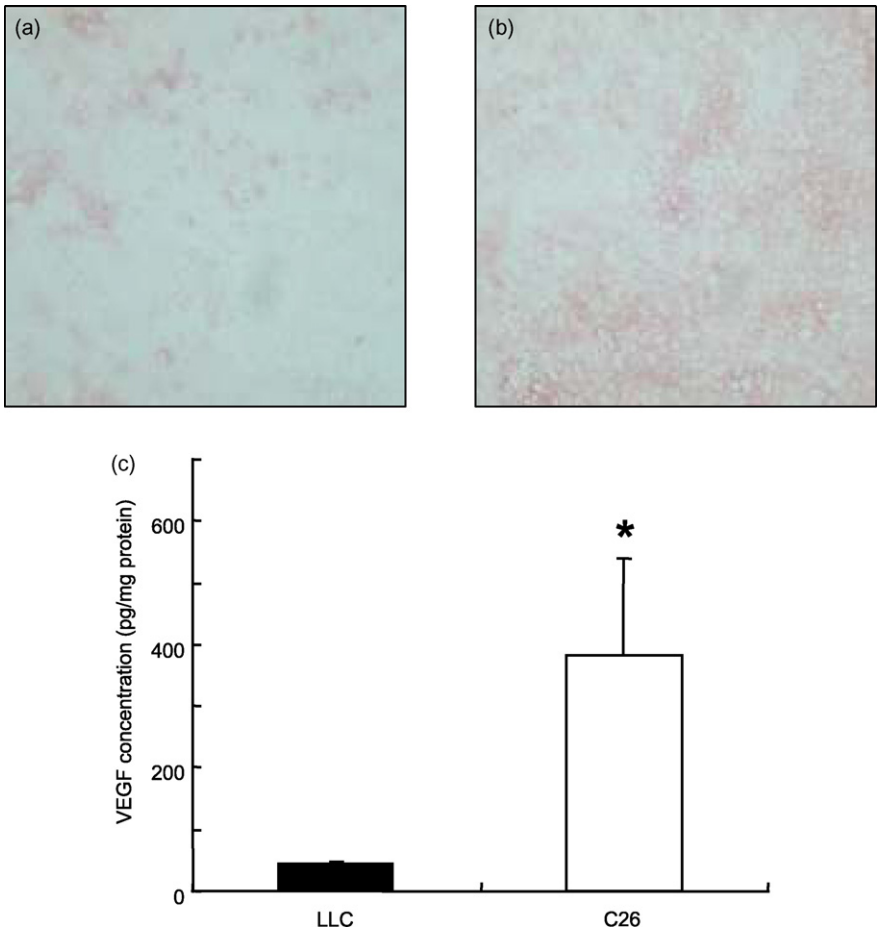

Fig. 6. Immunohistochemical staining of VEGF in LLC (a) and C26 tumors (b), and quantification of VEGF amount within the tumor tissue by ELISA (c). Tumor tissues were excised from mice when the tumor became 500 mm^3 in volume and were snap-frozen. Acetone-fixed 5-μm thick sections of tumor tissues were prepared and then AEC staining was performed for VEGF as described in Section 2. In parallel, tumor tissues were homogenized in lysis buffer containing 5% protease inhibitor cocktail and VEGF levels were quantified with commercially available ELISA kit. Results are expressed as the mean with the vertical bar showing S.D. of four independent experiments. $^*p < 0.05$, compared with LLC.

The present study clearly demonstrated that besides the improvement of retention of liposomal DOX in plasma, the higher vascular permeability within tumor tissues would also be required for liposomal DOX to be taken up more efficiently by tumor cells, indicating that the permeability of vasculature within tumor tissues is a critical factor for EPR effect-based anti-tumor effect of liposomal DOX.

References

Amice, J., Dazord, L., Toujas, L., 1978. Impairment of inflammatory reactions in tumour-bearing mice as measured by Evans blue extravasation. Eur. J. Cancer 14, 1287–1289.

Clasen, R.A., Pandolfi, S., Hass, G.M., 1970. Vital staining, serum albumin and the blood-brain barrier. J. Neuropathol. Exp. Neurol. 29, 266–284.

Dreher, M.R., Liu, W., Michelich, C.R., Dewhirst, M.W., Yuan, F., Chilkoti, A., 2006. Tumor vascular permeability, accumulation, and penetration of macromolecular drug carriers. J. Natl. Cancer Inst. 98, 335–344.

Eghbali, M., Birnir, B., Gage, P.W., 2003. Conductance of $GABA_A$ channels activated by pentobarbitone in hippocampal neurons from newborn rats. J. Physiol. 552, 13–22.

Gabizon, A.A., 1995. Liposome circulation time and tumor targeting: Implications for cancer chemotherapy. Adv. Drug Del. 16, 285–294.

Gabizon, A.A., Chemla, M., Tzemach, D., Horowitz, A.T., Goren, D., 1996. Liposome longevity and stability in circulation: effects on the in vivo delivery to tumors and therapeutic efficacy of encapsulated anthracyclines. J. Drug Target. 3, 391–398.

Gabizon, A.A., Shmeeda, H., Zalipsky, S., 2006. Pros and cons of the liposome platform in cancer drug targeting. J. Liposome Res. 16, 175–183.

Graff, B.A., Bjornaes, I., Rofstad, E.K., 2000. Macromolecule uptake in human melanoma xenografts: relationships to blood supply, vascular density, microvessel permeability and extracellular volume fraction. Eur. J. Cancer 36, 1433–1440.

Graff, B.A., Bjonaes, I., Rofstad, E.K., 2001. Microvascular permeability of human melanoma xenografts to macromolecules: relationships to tumor volumetric growth rate, tumor angiogenesis and VEGF expression. Microvascular Res. 61, 187–198.

Haran, G., Cohen, R., Bar, L.K., Barenholz, Y., 1993. Transmembrane ammonium sulfate gradient in liposomes produce efficient and stable entrapment of amphipathic weak bases. Biochim. Biophys. Acta 1151, 201–215.

Heyes, J., Hall, K., Tailor, V., Lenz, R., MacLachlan, I., 2006. Synthesis and characterization of novel poly(ethylene glycol)-lipid conjugates suitable for use in drug delivery. J. Control. Release 112, 280–290.

Kliche, S., Waltenberger, J., 2001. VEGF receptor signaling and endothelial function. IUBMB Life 52, 61–66.

Kratzke, R.A., Kramer, B.S., 1996. Evaluation of in vitro chemosensitivity using human lung cancer cell lines. J. Cell Biochem. 24, 160–164.

Lee, E.S., Na, K., Bae, Y.H., 2005. Doxorubicin loaded pH-sensitive polymeric micelles for reversal of resistant MCF-7 tumor. J. Control. Release 103, 405–418.

Lim, J.G., Lee, H.Y., Yun, J.E., Kim, S.P., Park, J.W., Kim, S.S., Han, J., Park, M.J., Song, D.K., 2004. Taurine block of cloned ATP-sensitive K^+ channels with different sulfonylurea receptor subunits expressed in *Xenopus laevis* oocytes. Biochem. Pharmacol. 68, 901–910.

Maeda, H., Wu, J., Sawa, T., Matsumura, Y., Hori, K., 2000. Tumor vascular permeability and the EPR effect in macromolecular therapeutics: a review. J. Control. Release 65, 271–284.

Mayer, L.D., Tai, L.C., Ko, D.S., Masin, D., Ginsberg, R.S., Cullis, P.R., Bally, M.B., 1989. Influence of vesicle size, lipid composition, and drug-to-lipid ratio on the biological activity of liposomal doxorubicin in mice. Cancer Res. 49, 5922–5930.

Mosmann, T., 1983. Rapid colorimetric assay for cellular growth and survival: application to proliferation and cytotoxicity assays. J. Immunol. Methods 65, 55–63.

Nakamura, R., Saikawa, Y., Kubota, T., Kumagai, A., Kiyota, T., Ohashi, M., Yoshida, M., Otani, Y., Kumai, K., Kitajima, M., 2006. Role of the MTT chemosensitivity test in the prognosis of gastric cancer patients after postoperative adjuvant chemotherapy. Anticancer Res. 26, 1433–1437.

Northfelt, D.W., Dezube, B.J., Thommes, J.A., Miller, B.J., Fischl, M.A., Friedman-Kien, A., Kaplan, L.D., Mond, C.D., Mamelok, R.D., Henry, D.H., 1998. Pegylated-liposomal doxorubicin versus doxorubicin, bleomycin, and vincristine in the treatment of AIDS-related Kaposi's sarcoma: results of a randomized phase III clinical trial. J. Clin. Oncol. 16, 2445–2451.

Roberts, W.G., Hasan, T., 1993. Tumor-secreted vascular permeability factor/vascular endothelial growth factor influences photosensitizer uptake. Cancer Res. 53, 153–157.

Schmidt, P.G., Adler-Moore, J.P., Forssen, E.A., Proffit, R.T., 1998. Unilamellar liposomes for anticancer and antifungal therapy. In: Lasic, D.D., Papahadjopoulos, D. (Eds.), Medical Applications of Liposomes. Elsevier Science BV, New York, pp. 703–731.

Shaw, G.L., Gazdar, A.F., Phelps, R., Steinberg, S.M., Linnoila, R.I., Johnson, B.E., Oie, H.K., Russell, E.K., Ghosh, B.C., Pass, H.I., Minna, J.D., Mulshine, J.L., Ihde, D.C., 1996. Correlation of in vitro drug sensitivity testing results with response to chemotherapy and survival: comparison of non-small cell lung cancer and small cell lung cancer. J. Cell Biochem. 24, 173–185.

Smit, E.F., de Vries, E.G., Timmer-Bosscha, H., de Leij, L.F., Oosterhuis, J.W., Scheper, R.J., Weening, J.J., Postmus, P.E., Mulder, N.H., 1992. In vitro response of human small-cell lung-cancer cell lines to chemotherapeutic drugs; no correlation with clinical data. Int. J. Cancer 51, 72–78.

Tanaka, S., Akaike, T., Wu, J., Fang, J., Sawa, T., Ogawa, M., Beppu, T., Maeda, H., 2003. Modulation of tumor-selective vascular blood flow and extravasation by the stable prostaglandin 12 analogue beraprost sodium. J. Drug Target 11, 45–52.

Tonn, J.C., Schachenmayr, W., Kraemer, H.P., 1994. In vitro chemosensitivity test of malignant gliomas: clinical relevance of test results independent of adjuvant chemotherapy. Anticancer Res. 14, 1371–1375.

Unezaki, S., Maruyama, K., Hosoda, J.I., Nagae, I., Koyanagi, Y., Nakata, M., Ishida, O., Iwatsuru, M., Tsuchiya, S., 1996. Direct measurement of the extravasation of polyethyleneglycol-coated liposomes into solid tumor tissue by in vivo fluorescence microscopy. Int. J. Pharm. 144, 11–17.

Yamaoka, K., Tanigawa, Y., Nakagawa, T., Uno, T., 1981. A pharmacokinetic analysis program (MULTI) for microcomputer. J. Pharmacobio-Dyn. 4, 879–885.

Yuan, F., Dellian, M., Fukumura, D., Leunig, M., Berk, D.A., Torchilin, V.P., Jain, R.K., 1995. Vascular permeability in a human tumor xenograft: molecular size dependence and cutoff size. Cancer Res. 55, 3752–3756.